# Direct observation in solution of a preexisting structural equilibrium for a mutant of the allosteric aspartate transcarbamoylase

**Luc Fetler*†, Evan R. Kantrowitz‡, and Patrice Vachette§¶**

*Centre de Recherche, Institut Curie, F-75248 Paris, France; †Laboratoire Physico-Chimie, Centre National de la Recherche Scientifique, Unité Mixte de Recherche 168, F-75248 Paris, France; ‡Department of Chemistry, Boston College, Merkert Chemistry Center, Chestnut Hill, MA 02467; and §Institut de Biochimie et Biophysique Moléculaire et Cellulaire, Unité Mixte de Recherche 8619, Centre National de la Recherche Scientifique, Université Paris-Sud, Bâtiment 430, F-91405 Orsay Cedex, France

Edited by Axel T. Brunger, Stanford University, Stanford, CA, and approved November 13, 2006 (received for review September 1, 2006)

**Many signaling and metabolic pathways rely on the ability of some of the proteins involved to undergo a substrate-induced transition between at least two structural states. Among the various models put forward to account for binding and activity curves of those allosteric proteins, the Monod, Wyman, and Changeux model for allostery theory has certainly been the most influential, although a central postulate, the preexisting equilibrium between the low-activity, low-affinity quaternary structure and the high-activity, high-affinity quaternary structure states in the absence of substrates, has long awaited direct experimental substantiation. Upon substrate binding, allosteric *Escherichia coli* aspartate transcarbamoylase adopts alternate quaternary structures, stabilized by a set of interdomain and intersubunit interactions, which are readily differentiated by their solution x-ray scattering curves. Disruption of a salt link, which is observed only in the low-activity, low-affinity quaternary structure, between Lys-143 of the regulatory chain and Asp-236 of the catalytic chain yields a mutant enzyme that is in a reversible equilibrium between at least two states in the absence of ligand, a major tenet of the Monod, Wyman, and Changeux model. By using this mutant as a magnifying glass of the structural effect of ligand binding, a comparative analysis of the binding of carbamoyl phosphate (CP) and analogs points out the crucial role of the amine group of CP in facilitating the transition toward the high-activity, high-affinity quaternary state. Thus, the cooperative binding of aspartate in aspartate transcarbamoylase appears to result from the combination of the preexisting quaternary structure equilibrium with local changes induced by CP binding.**

enzyme regulation | homotropic cooperativity | induced fit | intersubunit interactions | small-angle x-ray scattering

Many cellular responses, such as cell signaling, cell movements, intermediary metabolism, and the selective expression of genes, rely on the capacity of proteins to switch between different stable conformations in a reversible manner (1). Crystallographic studies have shown that, in agreement with the Monod, Wyman, and Changeux model for allostery theory (MWC) (2), most such proteins are made up of a finite number of identical subunits regularly organized around symmetry axes, which increases the stability of their conformational states and enhances the abrupt, switch-like character of their quaternary-structure transition between a low-activity, low-affinity (T) state and a high-activity, high-affinity (R) state (3). A critical statement of the MWC was that this conformational transition involves states that are populated in the absence of ligand and may spontaneously interconvert, the ligand stabilizing the conformation to which it binds with higher affinity. Initially, these concepts were developed based on catalytic activity measurements performed with regulatory enzymes, such as aspartate transcarbamoylase from *Escherichia coli* (ATCase). Most of these data can be interpreted by using the simple algebraic expressions of the MWC model, although some of the basic statements have long remained unproven. Regarding the quaternary structure, different conformations in either the absence or the presence of substrates have been described for a number of regulatory enzymes (4). A striking observation was that of a regular 1:1 complex of T- and R-state L-lactate dehydrogenase tetramers within the same crystal lattice (5). However, both T and R forms were complexed with ligands, substrates (NADH for T-state, NADH and pyruvate for R-state) and allosteric activator fructose 1,6-bisphosphate. Up to now, no formal thermodynamic and structural proof has been presented of the existence of an equilibrium between different structures in the absence of substrates. The closest approach was the study of spontaneous activity of an unliganded acetylcholine receptor channel from which a structural equilibrium was inferred but not observed (6). We report here a structural study in solution of a mutant form of an allosteric enzyme that we show to be, in the absence of ligands, in a reversible equilibrium between two quaternary structures with the two species existing in approximately equal concentrations.

Aspartate transcarbamoylase (EC 2.1.3.2) catalyzes the first step of pyrimidine biosynthesis, the condensation of CP and L-aspartate to form *N*-carbamoyl-L-aspartate (7). *E. coli* ATCase (306 kDa) is composed of two catalytic trimers carrying the six active sites and three regulatory dimers to which nucleotide effectors bind (see reviews in refs. 8 and 9), assembled with an approximate $D_3$ symmetry. ATCase exhibits homotropic cooperativity for aspartate binding in the presence of saturating amounts of CP, is activated by ATP and feedback inhibited by CTP (7) and UTP in the presence of CTP (10). Two functional and structural states of the enzyme have been characterized by a variety of techniques: a less active, low-affinity, T-state, stabilized by CTP and a more active, high-affinity, R-state stabilized by the substrates or the bisubstrate analog *N*-phosphonacetyl-L-aspartate (PALA). The corresponding crystal structures (11, 12) recently refined (13, 14) described the T-to-R transition as an 11-Å (1 Å = 0.1 nm) expansion along the 3-fold

Author contributions: L.F. and P.V. designed research; L.F. and P.V. performed research; E.R.K. contributed new reagents/analytic tools; L.F. and P.V. analyzed data; and L.F. and P.V. wrote the paper.

The authors declare no conflict of interest.

This article is a PNAS direct submission.

Abbreviations: ATCase, aspartate transcarbamoylase (aspartate carbamoyltransferase) from *E. coli* (EC 2.1.3.2.); CP, carbamoyl phosphate; PALA, *N*-(phosphonacetyl)-L-aspartate; T, low-activity, low-affinity quaternary structure state; R, high-activity, high-affinity quaternary structure state; MWC model, Monod, Wyman, and Changeux model for allostery; SAXS, small-angle X-ray scattering.

¶To whom correspondence should be addressed. E-mail: patrice.vachette@ibbmc.u-psud.fr.

This article contains supporting information online at www.pnas.org/cgi/content/full/0607641104/DC1.

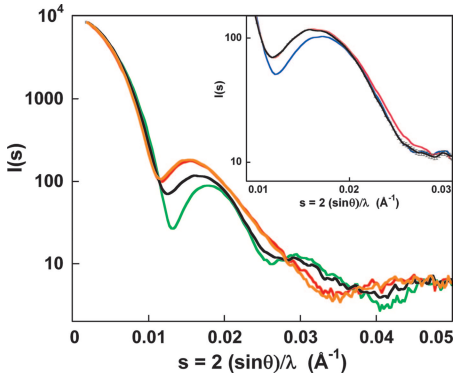


**Fig. 1.** Solution x-ray scattering spectra of wild-type and D236A ATCase. Green, unliganded wild-type enzyme; black, unliganded D236A ATCase; red, wild-type enzyme in the presence of a 2-fold molar excess of PALA; orange, D236A ATCase in the presence of a 2-fold molar excess of PALA. (*Inset*) Solution x-ray scattering spectrum of the D236A ATCase with experimental error bars and linear combinations of wild-type enzyme extreme patterns. Black, unliganded D236A enzyme; magenta, 56% T-44% R; blue, 76% T-24% R.

axis together with subunit and domain rotations (15) resulting in disruption of the r1-c4 interface between regulatory and catalytic chains. This quaternary rearrangement is accompanied by tertiary changes in both the catalytic and regulatory chains, most notably the 80s and 240s loops of the catalytic chains. Subsequently, small-angle X-ray scattering (SAXS) studies in solution showed that although the T conformation was practically identical in solution and in the crystal, major differences were observed in the R conformation (16). By using rigid-body modeling, a model for the R conformation in solution designated $R_{sol}$ was proposed in which the distance between the two catalytic trimers is 2.8 Å larger than in the crystal structure, whereas both catalytic and regulatory subunits undergo rotations of greater amplitudes than in the crystal around their local symmetry axes (16, 17).

The salt bridge that Asp-236 of the catalytic chain forms in the T structure with Lys-143*r* from the neighbor regulatory chain within the so-called c1-r4 interface was first reported in the crystal structure of the complex of the enzyme with phosphonacetamide (18) and in the structure of unliganded E239Q-ATCase (19). This interface is not observed in the R structure (12, 14, 15), but this specific salt link is also absent in the crystal structure of ATCase complexed with ATP (9). This ionic interaction is thought to play a crucial role in the stabilization of the low-activity T structure and, therefore, in the regulatory properties of the enzyme. Replacement of Asp-236 by an alanine residue yields a mutant enzyme (D236A ATCase), reported to exhibit much reduced cooperativity for aspartate, if any (20, 21) whereas its activity is not modulated by nucleotide effector binding. Equilibrium isotope exchange kinetics and kinetic isotope effect studies have shown that the mutant enzyme operates by the same ordered kinetic mechanism as the wild-type enzyme, i.e., CP binding before aspartate (21).

## Results and Discussion

**X-Ray Scattering Spectra of Unliganded and PALA Saturated Enzymes.** The small-angle x-ray scattering pattern of unliganded D236A ATCase differs from the scattering pattern of the wild-type enzyme: the intensities in the region of the first subsidiary minimum and maximum are closer to the wild-type R curve than to the T curve, whereas, at larger *s* values, the intensities of the unliganded D236A ATCase scattering profile are closer to the wild-type T curve (Fig. 1). In contrast, the scattering pattern of the mutant enzyme in the presence of saturating PALA is nearly identical to the wild-type R pattern, indicating that the mutant enzyme still undergoes a structural transition, although reduced, upon PALA binding. Addition of 30% PALA, expressed as the fraction of occupied active sites, to the D236A ATCase yields a scattering pattern identical to the R pattern (data not shown). Even in the presence of only 10% PALA, a concentration for which the wild-type enzyme is in a 90% T–10% R equilibrium, D236A ATCase shows a much larger change toward R state, with approximately half of the molecules in the R state (data not shown). Clearly, D236A ATCase is more readily converted to the R quaternary structure upon addition of a low amount of PALA than the wild-type enzyme.

As already reported (22), the scattering curve of the unliganded D236A ATCase cannot be approximated by a linear combination of the wild-type T and R curves. Indeed, a 56% T–44% R linear combination of the wild-type T and R patterns fits well the region of the first minimum and maximum but fails in the [0.022 Å$^{-1}$ to 0.03 Å$^{-1}$] region (the root-mean-square value of reduced residuals in this range is 3.3), which requires a 76% T–24% R combination [Fig. 1 (*Inset*), magenta and blue curves, respectively]. This result indicates conclusively that the solution of the unliganded mutant is not a mixture of T and R structures. The scattering pattern of the unliganded D236A ATCase can be accounted for in two ways. Either the unliganded D236A ATCase adopts a new quaternary structure, different from both the wild-type T and R structures, or the solution of the unliganded D236A ATCase is a mixture of at least two structures, one of which is different from both wild-type T and R structures.

**Effect of Nucleotide Addition.** The mutant enzyme is easily converted into the R conformation by addition of low concentrations of PALA. Are there conditions under which the T conformation would be predominant, or is this low-activity conformation inaccessible to the D236A ATCase? From previous work with the wild-type enzyme, it is known that addition of CTP, an allosteric inhibitor of the enzyme, shifts the T to R equilibrium by approximately 6–8% toward the T structure from a roughly equal concentration of the T and R states obtained in the presence of a subsaturating concentration of PALA (23). We therefore studied the effect of CTP on the unliganded mutant enzyme. The resulting scattering pattern is T shifted and appears to be very close to the T pattern, (Fig. 2*A*), indicating that most of the mutant molecules are in the T conformation. Similar results have been obtained in the presence of UTP or CTP/UTP (data not shown), showing that although the T state has been dramatically destabilized by the mutation, it remains accessible to D236A ATCase upon inhibitor binding. This result is suggestive of a weakened energy barrier between conformations with enhanced effects of ligand binding on the equilibrium. Interestingly, the addition of ATP causes no change in the scattering curve other than a small filling up of the first subsidiary minimum (Fig. 2*A*) that is due to ATP binding *per se*, i.e., the contribution of ATP to the scattering and does not involve any quaternary structure change, as observed with the wild-type enzyme (17). This absence of effect is in sharp contrast to the enhanced effect of CTP.

Mg-ATP, the prevailing form of ATP *in vivo*, has been shown to have a different effect on the quaternary structure of the wild-type enzyme than ATP. A previous SAXS study demonstrated that Mg-ATP binding, although it does not alter the T to R equilibrium, modifies the solution structure of the PALA-bound enzyme to a more extended conformation designated $R_{sol+Mg\text{-}ATP}$, which we have modeled using rigid-body movements of subunits (17). The distance between the two catalytic trimers is 1.6 Å larger than that in the solution structure of PALA-bound ATCase. The scattering pattern of D236A ATCase has been recorded in the presence of both saturating PALA and 5 mM Mg-ATP and is practically identical to that of the

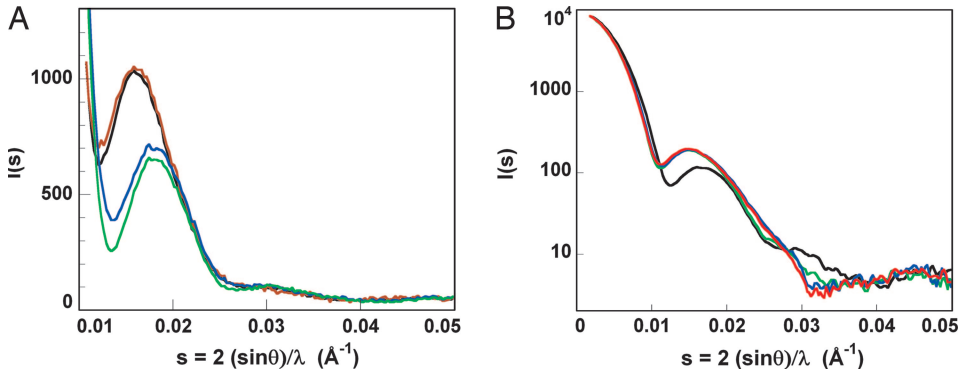


**Fig. 2.** Solution x-ray scattering spectra of D236A ATCase in the presence of nucleotide effectors. (*A*) pH 8.3. Black, unliganded D236A ATCase; brown, D236A ATCase + 5 mM ATP; blue, D236A ATCase + 5 mM CTP; green, unliganded wild-type ATCase (T-state). (*B*) pH 7. Black, unliganded D236A ATCase; green, D236A ATCase + 5 mM Mg-ATP; red, PALA-bound D236A ATCase + 5 mM Mg-ATP; blue, PALA-bound wild-type ATCase + 5 mM Mg-ATP.

wild-type enzyme under the same conditions as shown in Fig. 2*B*. More interestingly, addition of Mg-ATP alone to the unliganded enzyme is enough to yield a very similar scattering pattern (Fig. 2*B*), suggesting that nearly all molecules are in the $R_{sol+Mg\text{-}ATP}$ extended conformation. This is in marked contrast to the unliganded wild-type enzyme whose quaternary structure is unaffected by Mg-ATP binding (17). In summary, the scattering pattern (quaternary structure distribution) of the D236A ATCase appears to be very sensitive to ligand binding, be it a bisubstrate analog such as PALA or nucleotide effectors such as CTP (inhibitor) or Mg-ATP (activator).

**Direct Evidence of a Thermodynamic Equilibrium Between Different Conformations.** To test the hypothesis that the unliganded enzyme is in equilibrium between different conformations, as postulated by the MWC model, scattering patterns of both the unliganded mutant and wild-type enzymes were recorded as a function of temperature. Whereas the wild-type curve displays no significant variation up to 55°C before exhibiting clear signs of dissociation at 60°C (Fig. 3*A*), the pattern of the D236A ATCase undergoes a clear T shift when the temperature increases from 6–30°C (purple to yellow curves in Fig. 3*B*) before partially reverting toward R between 30°C and 45°C (yellow to red curves in Fig. 3*B*). In this temperature range, the variation is reversible, as shown by the pair of curves recorded at 15°C and 20°C during the heating and cooling phases, curves which are identical within experimental errors (Fig. 3*C*). The temperature dependence of the quaternary structure equilibrium is not monotonous but exhibits an extremum at ≈30°C. This shows that more than one process is at work, a complexity that precludes a quantitative analysis of the data.

We wish to emphasize that the observation of reversible changes in the scattering pattern of the unliganded D236A ATCase is the first direct proof of the existence of such an equilibrium. It is therefore a crucial result, albeit bearing on a mutant enzyme rather than on the wild-type molecule, for which the equilibrium is too strongly shifted toward T to allow the detection of a very small fraction of molecules in the R conformation (of the order of 1% because $L = 250$ (24) or $L = 70$ (23), where $L$ is the allosteric constant $L = [T_0]/[R_0]$ in the absence of substrate). Previous sedimentation velocity measurements were interpreted by assuming this equilibrium, although the very careful analysis of boundary spreading in this kind of experiment by the same authors were clearly in favor of a two-state transition (25). Similarly, our previous SAXS titration studies of the transition using PALA, alone or in the presence of the first substrate or nucleotide effectors, as well as time-resolved SAXS studies of the transition, also led us to conclude firmly to the existence of a concerted transition between T and R conformations (23, 26–28). However, to date, there had been no direct proof of the existence of the structure equilibrium for an unliganded enzyme, i.e., of the accessibility of an R-like structure to an unliganded enzyme.

**Consequences of Substrate Binding.** The low activation energy of the quaternary structure transition endows the D236A ATCase with a significantly enhanced sensitivity to ligand binding. This enhanced sensitivity operates as a magnifying glass to monitor the structural effect of ligand binding as already illustrated by the

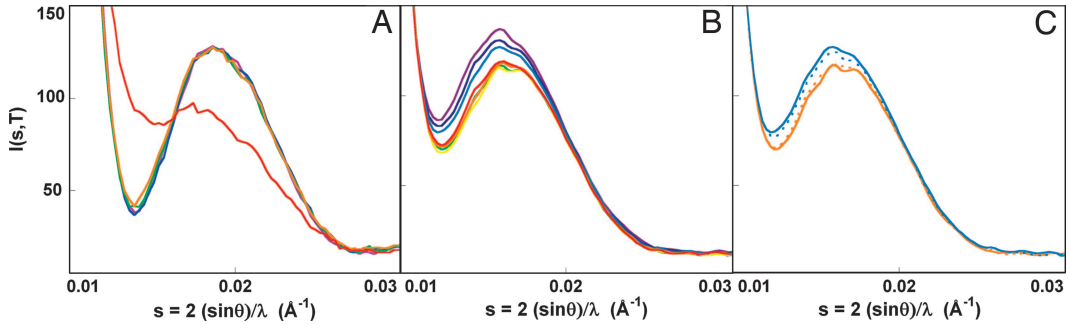


**Fig. 3.** Effect of temperature on both wild-type and D236A unliganded ATCases. (*A*) SAXS patterns of unliganded wild-type ATCase recorded at temperatures ranging from 4°C (dark blue) to 60°C (red). (*B*) SAXS patterns of unliganded D236A ATCase at temperatures ranging from 6°C (dark blue) to 45°C (red). (*C*) Reversibility of the temperature effect on the unliganded D236A ATCase. Scattering patterns recorded at 15°C (blue) and 20°C (orange) during the heating (continuous line) and cooling (dashed line) phases.

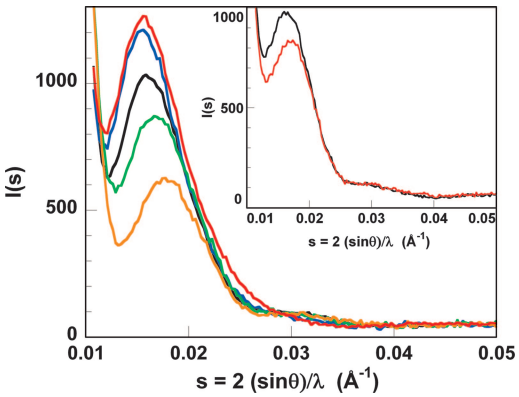


**Fig. 4.** Solution x-ray scattering spectra of the D236A ATCase in the presence of the first substrate, CP, and its analogs. Black, unliganded D236A ATCase; blue, D236A ATCase + 5 mM CP; red, D236A ATCase + 2-fold molar excess of PALA; green, D236A ATCase + 5 mM *N*-methyl-carbamoyl phosphate; orange, D236A ATCase + 5 mM acetyl phosphate. (*Inset*) black, unliganded D236A ATCase; red, D236A ATCase + 100 mM aspartate.

large alterations in the SAXS pattern when PALA, CTP, and Mg-ATP bind. We have therefore undertaken a systematic study of ligand binding, the results of which are summarized in supporting information (SI) Table 1. We will comment here on only a few selected observations of direct relevance for the regulatory properties of the enzyme.

**Effect of CP and Analogs.** Upon CP binding, the scattering pattern is close to the R pattern (Fig. 4), showing that the vast majority of enzyme molecules are in an R-like conformation in the presence of only the first substrate, in agreement with a recent observation (29). This effect of CP alone explains the absence of cooperativity for aspartate binding, as already reported for the E239Q-ATCase (30) and the K143*r*A-ATCase (31). This observation is easily understood in the context of a destabilized T state but is at variance with a model put forward by the authors of earlier equilibrium isotope exchange kinetics studies, in which aspartate induces the initial conformational changes in a rate-limiting step that, in turn, triggers the T-to-R transition (21).

Three CP analogs: acetyl phosphate, *N*-methyl-carbamoyl phosphate and phosphonacetamide were also studied. The first two have been shown to bind to the active site of wild-type catalytic subunit, although with a weaker affinity (32) and are substrates in the presence of aspartate, although less effective than CP. Surprisingly, both acetyl phosphate and *N*-methyl-carbamoyl phosphate cause alterations of the scattering pattern of the D236A ATCase opposite to those observed with CP. Indeed, the scattering pattern in the presence of *N*-methyl-carbamoyl phosphate or acetyl phosphate is shifted toward the wild-type T curve (Fig. 4), this T shift being largest with acetyl phosphate. In contrast, phosphonacetamide has no effect on the scattering pattern of the D236A ATCase (Table 1), similar to the observation with the wild-type enzyme. Interestingly, D236A ATCase has been crystallized in the presence of phosphonacetamide, and the enzyme appears to be in the R conformation, at variance with our observation in solution (29). However, crystals were grown in different conditions that might have favored the R-quaternary structure. The comparison between the chemical formula of the four compounds points toward the amine group as playing a key role in mediating the structural effect of the first ligand binding. Although phosphonacetamide possesses an amine group, the replacement of the oxygen atom by a methylene group probably suffices to alter its interactions with the surrounding amino acids within the active site. In the recently published structure of the complex of ATCase with CP (13), the amine group is seen to interact with the main chain carbonyls of Pro-266 and Leu-267 and with the side-chain carbonyl of Gln-137. In solution, Q137A-ATCase does not undergo the quaternary structure transition in the presence of both CP and aspartate (33), most likely because CP binds in an incorrect orientation. The interactions with residues 266 and 267 involve main chain atoms and are therefore difficult to test by site-directed mutagenesis. Actually, Pro-268, next to Pro-266 and Leu-267 has been mutated to an alanine (34). The mutant enzyme exhibits altered catalytic and regulatory properties, with much reduced activity and cooperativity together with a weaker affinity for both substrates, whereas the structure exhibits only local differences of small amplitudes. Taken together, our observations and these results suggest that the link between the amine group of CP and the carbonyl of Gln-137 is the primary interaction leading to the T-state destabilization caused by CP binding, with likely contributions from the other two links with the main chain carbonyls of Pro-266 and Leu-267.

**Effect of Aspartate and Analogs and Combinations Thereof.** Aspartate and three analogs were assayed for their effect on the solution structure of the enzyme. Although none has any significant effect on the wild-type enzyme, all substrates cause a marked T shift of the scattering pattern (Fig. 4 *Inset*), an unexpected outcome. Indeed, according to the linkage equations of Wyman (35, 36), it follows that aspartate and its analogs have higher affinity for the T state than for the R state of ATCase, a result difficult to reconcile with the fact that the wild-type enzyme exhibits cooperative aspartate binding. In a recently reported *in silico* docking study, CP and aspartate were found to bind in strongly overlapping positions within the active site of the unliganded wild-type enzyme (13). Only in the presence of CP does aspartate bind productively. Both results underline the role of CP in preparing the active site for aspartate binding, because it appears that the homotropic cooperativity for aspartate binding is a specific property of the CP–ATCase complex. In other words, the ordered substrate binding, established for both the mutant and the wild-type enzymes, is part of the mechanism for homotropic cooperativity.

**Quaternary Structures.** Our direct observation of a structure equilibrium for the unliganded D236A ATCase leaves open the question of the unknown conformation explored by the enzyme. Our attempts at fitting the unliganded D236A ATCase scattering pattern by a linear combination of the wild-type T and R patterns required a smaller fraction of T (0.56) in the region of the first minimum and maximum than at larger angles (0.76). The scattering pattern of a conformation more expanded along the threefold axis exhibits a subsidiary minimum and maximum shifted to smaller angles (e.g., compare unliganded and PALA-bound patterns in Fig. 1 or PALA-bound and PALA + Mg-ATP bound patterns in Fig. 2). The position of the maximum results essentially from the average distance between the two catalytic trimers , whereas intensities are also sensitive to their relative orientation. Clearly, the involvement of a more expanded conformation than R would yield an increase of the T fraction required for a fit around the first minimum and maximum.

First, such an extended conformation has already been observed in the presence of Mg-ATP. We tried therefore to fit the unliganded D236A ATCase scattering pattern by a linear combination of the scattering patterns of the unliganded wild-type ATCase (T conformation) and Mg-ATP-bound D236A ATCase. A good agreement was obtained by using a linear combination of 62% unliganded wild-type ATCase (T conformation) and 38% Mg-ATP-bound D236A ATCase (red curve in Fig. 5).

Secondly, the quaternary structure of the wild-type enzyme in the presence of both PALA and Mg-ATP ($R_{sol+MgATP}$) has been modeled by using rigid body movements of the two catalytic

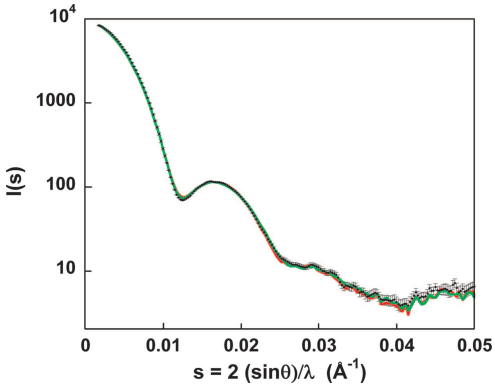


**Fig. 5.** Fitting of the unliganded D236A ATCase scattering pattern. Black, experimental SAXS pattern of the unliganded D236A ATCase with experimental error bars; red, linear combination of 62% T-38% Mg-ATP-bound D236A ATCase; green, linear combination of 63% T-37% $R_{sol+MgATP}$.

trimers and of the three regulatory dimers (17). In this conformation, the distance between catalytic trimers is 4.4 Å larger with respect to $R_{cry}$ as compared with 2.8 Å for $R_{sol}$. We calculated the scattering pattern of the $R_{sol+MgATP}$ conformation and attempted to fit the pattern of unliganded D236A ATCase by a linear combination of this extended conformation and of the T pattern (unliganded wild-type enzyme). A very satisfactory fit to the data was obtained by combining 63% T and 37% $R_{sol+MgATP}$ (green curve in Fig. 5).

Both results therefore suggest that the unliganded D236A ATCase is in equilibrium with essentially even concentrations of the T conformation and the Mg-ATP-bound conformation. This finding is indirectly supported by equilibrium exchange and kinetic isotope effect studies showing that the kinetic behavior of the D236A ATCase, although not identical, appears to be closest to that of the ATP-bound wild-type enzyme (21).

Studying the related mutant K143*r*A, which exhibits similarly noncooperative aspartate binding and no response to nucleotide effectors, Schachman and collaborators interpreted the corresponding sedimentation velocity measurements in terms of equilibrium between T and R conformations (31). Our conclusion regarding the D236A ATCase is similar, but, with two significant differences. First, we observe the direct effect of the conformation equilibrium on the SAXS pattern together with its reversibility. Second, thanks to the high structural information content of SAXS patterns (see *Materials and Methods*), we show that linear combinations of T and R (PALA-bound) patterns cannot account for the unliganded pattern of the mutant enzyme, and therefore the equilibrium involves a different conformation that we characterize.

## Conclusion

Suppressing the salt link between Asp-236 of the catalytic chain and Lys-143*r* destabilizes the T conformation of ATCase. As a consequence, the two quaternary structures postulated by Monod *et al.* (2) become almost equally populated, and we have been able to establish conclusively, using the temperature dependence of the equilibrium constant *L*, that the unliganded D236A ATCase is in a reversible equilibrium between different conformations. This is the first direct experimental proof of such a quaternary structure equilibrium for ATCase, albeit on a mutant form of the enzyme. We further propose that the equilibrium involves the T conformation and the Mg-ATP-bound conformation very close to the conformation dubbed $R_{sol+MgATP}$ of the wild-type enzyme.

It could be argued that the so-called Mg-ATP-bound conformation should be considered as the true R conformation involved in the T ↔ R quaternary equilibrium put forward by Monod *et al.* (2) in their model for allostery. However, from an enzymatic point of view, it is the CP–ATCase complex that exhibits homotropic cooperativity for aspartate binding, due to the ordered binding of substrates. The distinction is not purely academic if one considers that aspartate and its analogs appear to have higher affinity for the unliganded T state of the D236A ATCase than for the Mg-ATP-bound conformation. The regulation of ATCase activity appears therefore to involve a combination of preexisting quaternary structure equilibrium and local, small-amplitude induced fit upon substrate binding, which can, in turn, modulate the equilibrium. Such a notion has been put forward in recent studies of correlations between structural changes involved in ligand binding to protein and intrinsic motions of proteins in the unbound state as revealed by normal mode analysis (37, 38). It would now be of great interest to try and crystallize the unliganded mutant enzyme, in the hope that the $R_{sol+MgATP}$ conformation could be selectively crystallized and its high-resolution structure determined.

## Materials and Methods

**Chemicals and Enzyme Preparation.** ATP, CTP, CP, acetyl phosphate, *N*-methyl-carbamoyl phosphate, phosphonacetamide, *L*-cysteine sulfinate, succinate, and malonate were purchased from Sigma (St. Louis, MO) Tris(hydroxymethyl)aminomethane (Tris) was from Merck (Darmstadt, Germany). PALA was a generous gift from V. Narayanan and L. Kedda of the Drug Synthesis and Chemistry Branch, Division of Cancer Treatment, National Institutes of Health (Silver Spring, MD). Wild-type and D236A ATCases were isolated as described by Nowlan and Kantrowitz (39), from overproducing *E. coli* strain EK1104 [$F^-$ *ara*, *thi*, Δ*pro-lac*, Δ*pyrB*, *pyrF*$^{+/-}$, *rpsL*], containing the plasmid pEK17 (39) or pEK116 (20), respectively.

**Solution X-Ray Scattering.** X-ray scattering curves were recorded on the small-angle scattering instrument D24 by using synchrotron radiation at Laboratoire pour l'Utilisation du Rayonnement Electromagnétique (LURE), Orsay, France. The instrument, the data acquisition system (40), the evacuated measuring cell (41), and the experimental procedures (23) have already been described. Data were recorded over the angular range 0.01 $Å^{-1} < s < 0.05$ $Å^{-1}$, where $s = (2\sin\theta)/\lambda$ is the modulus of the scattering vector, $2\theta$ is the scattering angle, λ is the radiation wavelength (λ = 1.488 Å, absorption K-edge of Ni). For a few dilute samples, data were recorded down to $s_{min} = 0.0016$ $Å^{-1}$. Experiments were first recorded in 50 mM Tris·HCl at pH 8.3, conditions under which the cooperativity of the enzyme for aspartate binding is maximal (42). However, Tris buffer is known to exhibit a marked temperature dependence. The temperature dependence of the unliganded D236A ATCase scattering pattern was thus compounded by a putative pH effect. Therefore, experiments were also performed in 50 mM phosphate buffer, pH 7.0, which exhibits a temperature dependence of much reduced amplitude and of opposite sign. We have already shown that, in the case of the wild-type enzyme, the unliganded pattern and the PALA-bound pattern were identical at both pH values (17). The temperature dependence observed with the mutant enzyme is essentially identical to that obtained at pH 8.3. Therefore, we present here the temperature dependence and the effect of Mg-ATP binding at (constant) pH 7.0, whereas the studies of other ligand-binding effects, for which the temperature was kept constant (T = 20°C or 293 K), were performed at pH 8.3. All solutions contained 0.1 mM DTT to minimize radiation damage. Shortly before measurements, the purified enzyme solution was run through a size-exclusion HPLC column to eliminate aggregated material before concentration. The samples for x-ray scattering experiments were

prepared extemporaneously to a final protein concentration of 50 mg·ml$^{-1}$ (pH 8.3) and 25 mg·ml$^{-1}$ (pH 7.0), except for the smallest angle data recorded at 5 mg·ml$^{-1}$ (pH 8.3) and 2 mg·ml$^{-1}$ (pH 7.0). The concentration was determined by absorbance measurements at 280 nm by using an extinction coefficient of 0.59 cm$^2$·mg$^{-1}$ for ATCase (43). A 2-fold molar excess of the bisubstrate analog PALA ([PALA]/[active site]) was considered sufficient to saturate all active sites, in view of the high affinity of PALA for the active site [$K_D$ = 27 nM for the catalytic wild-type subunit (44)].

The intensity scattered by a noninteracting solution of protein is the sum of the intensities of all individual particles. In the case of a mixture of different particles, the resulting intensity is the sum of the contributions of each particle weighted by their fractional concentrations. Although performed in solution, like hydrodynamic experiments, SAXS measurements yield a greater amount of structural information in the sense of independent parameters needed to reconstruct scattering curves than the single parameter (e.g., the sedimentation coefficient) provided by hydrodynamic measurements. The scattering patterns of ATCase solutions presented here yield ≈14 independent Shannon parameters (17, 45, 46).

**Rigid-Body Modeling.** The rigid-body model of the expanded conformation observed in the presence of Mg-ATP has already been described (17). Briefly, the scattering intensities were computed from the crystallographic models by using the program CRYSOL (47). The coordinates of ATCase were taken from the Protein Data Bank (RCSB) (48) entry 1d09 (R state with PALA) (14). We applied to the catalytic trimers and to regulatory dimers of this structure the translations and rotations reported in ref. 17, which yield the best fit to the experimental scattering pattern in the presence of Mg-ATP ($R_{sol+Mg\text{-}ATP}$), i.e., $\Delta c$ = 2.2 Å and $\Delta\phi$ = 13° ($\Delta c$ is the translation of each catalytic trimer along the 3-fold axis and $\Delta\phi$ their rotation around the same axis) and $\Delta r$ = 1.8 Å and $\Delta\theta$ = 15° ($\Delta r$ is the translation of each regulatory dimer along the 2-fold axis, and $\Delta\theta$ is their rotation around the same axis).

We thank M. Renouard and C. Mérigoux for help with the final steps of sample preparation, P. Tauc for help at an early stage of this work, and the technical staff from LURE. This work was supported by the Centre National de la Recherche Scientifique (P.V.), the Institut National de la Santé et de la Recherche Médicale (L.F.), and National Institutes of Health Grant GM26237 (to E.R.K.).

1. Changeux JP, Edelstein SJ (2005) *Science* 308:1424–1428.
2. Monod J, Wyman J, Changeux JP (1965) *J Mol Biol* 12:88–118.
3. Perutz MF (1989) *Q Rev Biophys* 22:139–237.
4. Hervé G (1989) *Allosteric Enzymes* (CRC, Boca Raton, FL).
5. Iwata S, Kamata K, Yoshida S, Minowa T, Ohta T (1994) *Nat Struct Biol* 1:176–185.
6. Jackson MB (1986) *Biophys J* 49:663–672.
7. Gerhart JC, Pardee AB (1962) *J Biol Chem* 237:891–896.
8. Hervé G (1989) in *Allosteric Enzymes*, ed Hervé G (CRC, Boca Raton, FL), pp 61–79.
9. Lipscomb WN (1994) *Advan Enzymol* 68:67–152.
10. Wild JR, Loughrey-Chen SJ, Corder TS (1989) *Proc Natl Acad Sci USA* 86:46–50.
11. Ke H, Honzatko RB, Lipscomb WN (1984) *Proc Natl Acad Sci USA* 81:4037–4040.
12. Krause KL, Volz KW, Lipscomb WN (1987) *J Mol Biol* 193:527–553.
13. Wang J, Stieglitz KA, Cardia JP, Kantrowitz ER (2005) *Proc Natl Acad Sci USA* 102:8881–8886.
14. Jin L, Stec B, Lipscomb WN, Kantrowitz ER (1999) *Proteins* 37:729–742.
15. Ke H, Lipscomb WN, Cho Y, Honzatko RB (1988) *J Mol Biol* 204:725–748.
16. Svergun DI, Barberato C, Koch MH, Fetler L, Vachette P (1997) *Proteins* 27:110–117.
17. Fetler L, Vachette P (2001) *J Mol Biol* 309:817–832.
18. Gouaux JE, Lipscomb WN (1990) *Biochemistry* 29:389–402.
19. Gouaux JE, Stevens RC, Ke H, Lipscomb WN (1989) *Proc Natl Acad Sci USA* 86:8212–8216.
20. Newton CJ, Kantrowitz ER (1990) *Proc Natl Acad Sci USA* 87:2309–2313.
21. Wedler FC, Ley BW, Lee BH, O'Leary MH, Kantrowitz ER (1995) *J Biol Chem* 270:9725–9733.
22. Chan RS, Sakash JB, Macol CP, West JM, Tsuruta H, Kantrowitz ER (2002) *J Biol Chem* 277:49755–49760.
23. Fetler L, Tauc P, Hervé G, Moody MF, Vachette P (1995) *J Mol Biol* 251:243–255.
24. Howlett GJ, Schachman HK (1977) *Biochemistry* 16:5077–5083.
25. Werner WE, Schachman HK (1989) *J Mol Biol* 206:221–230.
26. Fetler L, Tauc P, Vachette P (1997) *J Appl Crystallogr* 30:781–786.
27. Tsuruta H, Kihara H, Sano T, Amemiya Y, Vachette P (2005) *J Mol Biol* 348:195–204.
28. Tsuruta H, Vachette P, Sano T, Moody MF, Amemiya Y, Wakabayashi K, Kihara H (1994) *Biochemistry* 33:10007–10012.
29. Stieglitz KA, Dusinberre KJ, Cardia JP, Tsuruta H, Kantrowitz ER (2005) *J Mol Biol* 352:478–486.
30. Tauc P, Vachette P, Middleton SA, Kantrowitz ER (1990) *J Mol Biol* 214:327–335.
31. Eisenstein E, Markby DW, Schachman HK (1990) *Biochemistry* 29:3724–3731.
32. Porter PW, Modebe MO, Stark GR (1969) *J Biol Chem* 244:1846–1859.
33. Stieglitz KA, Pastra-Landis SC, Xia J, Tsuruta H, Kantrowitz ER (2005) *J Mol Biol* 349:413–423.
34. Jin L, Stec B, Kantrowitz ER (2000) *Biochemistry* 39:8058–8066.
35. Wyman J (1967) *J Am Chem Soc* 89:2202–2218.
36. Wyman J (1964) *Adv Protein Chem* 19:223.
37. Tobi D, Bahar I (2005) *Proc Natl Acad Sci USA* 102:18908–18913.
38. Kong Y, Ma J, Karplus M, Lipscomb WN (2006) *J Mol Biol* 356:237–247.
39. Nowlan SF, Kantrowitz ER (1985) *J Biol Chem* 260:14712–14716.
40. Boulin C, Kempf R, Koch MHJ, McLaughlin SM (1986) *Nuclear Instrum Meth* A249:399–407.
41. Dubuisson JM, Decamps T, Vachette P (1997) *J Appl Crystallogr* 30:49–54.
42. Pastra-Landis SC, Evans DR, Lipscomb WN (1978) *J Biol Chem* 253:4624–4630.
43. Gerhart JC, Holoubek H (1967) *J Biol Chem* 242:2886–2892.
44. Collins KD, Stark GR (1971) *J Biol Chem* 246:6599–6605.
45. Luzatti V (1980) in *Imaging Processes and Coherence in Physics, Lecture Notes in Physics*, eds Schlenker M, Fink M, Goedgebuer JP, Malgrange C, Vienot JC, Wade R (Springer, New York), pp 209–215.
46. Koch MHJ, Vachette P, Svergun DI (2003) *Quart Rev Biophys* 36:147–227.
47. Svergun DI (1992) *J Appl Crystallogr* 25:495–503.
48. Berman HM, Westbrook J, Feng Z, Gilliland G, Bhat TN, Weissig H, Shindyalov IN, Bourne PE (2000) *Nucleic Acids Res* 28:235–242.